Platelet-Specific PDGFB Ablation Impairs Tumor Vessel Integrity and Promotes Metastasis

Yanyu Zhang[1], Jessica Cedervall[1], Anahita Hamidi[1], Melanie Herre[1], Kati Viitaniemi[2], Gabriela D'Amico[2], Zuoxiu Miao[1], Ragaseema Valsala Madhavan Unnithan[1,3], Alessandra Vaccaro[4], Luuk van Hooren[4], Maria Georganaki[4], Åsa Thulin[5], Qi Qiao[1], Johanna Andrae[4], Agneta Siegbahn[5], Carl-Henrik Heldin[1], Kari Alitalo[2], Christer Betsholtz[4,6], Anna Dimberg[4], and Anna-Karin Olsson[1]

ABSTRACT

Platelet-derived growth factor B (PDGFB) plays a crucial role in recruitment of PDGF receptor β–positive pericytes to blood vessels. The endothelium is an essential source of PDGFB in this process. Platelets constitute a major reservoir of PDGFB and are continuously activated in the tumor microenvironment, exposing tumors to the plethora of growth factors contained in platelet granules. Here, we show that tumor vascular function, as well as pericyte coverage is significantly impaired in mice with conditional knockout of PDGFB in platelets. A lack of PDGFB in platelets led to enhanced hypoxia and epithelial-to-mesenchymal transition in the primary tumors, elevated levels of circulating tumor cells, and increased spontaneous metastasis to the liver or lungs in two mouse models. These findings establish a previously unknown role for platelet-derived PDGFB, whereby it promotes and maintains vascular integrity in the tumor microenvironment by contributing to the recruitment of pericytes.

Significance: Conditional knockout of PDGFB in platelets demonstrates its previously unknown role in the maintenance of tumor vascular integrity and host protection against metastasis.

Introduction

The vasculature constitutes an essential barrier between the tissue parenchyma and the circulating blood and provides key signals to quickly recruit circulating blood cells to sites of injury, inflammation, and infection (1). In addition to the endothelial cells facing the lumen, blood vessels are composed of supporting (mural) cells attached to the abluminal side of the endothelium. Mural cells in capillaries, pericytes, help to maintain integrity of the vasculature, and diseases such as diabetic retinopathy and vascular malformations are characterized by pericyte loss (2–4). During development, proper pericyte recruitment to the vasculature is dependent on the interaction between platelet-derived growth factor B (PDGFB) expressed by the endothelium and PDGF receptor β (PDGFRβ) expressed by the pericytes (5–9). In addition, the endothelial-derived PDGFB must be anchored to the extracellular matrix (ECM) in close proximity to the vasculature, thereby creating a gradient that attracts PDGFRβ-expressing pericytes to form close attachments to the endothelium. This anchoring of PDGFB to the ECM is achieved by the "retention motif," which is a heparan sulfate–binding region in the C-terminal domain of the growth factor (10–12). In a tumor, pericytes are commonly less numerous and also less tightly attached to the endothelium (13, 14). There could be several explanations, such as loss of the PDGFB gradient due to expression of PDGFB by tumor cells also (11) and/or increased proteolytic activity in the tumor microenvironment, which could release PDGFB bound to the ECM, thereby disrupting the gradient. An imbalance between angiopoietin 1 (Ang1) and Ang2 signaling through the Tie2 receptor on endothelial cells can also affect pericyte coverage in tumor vasculature (15).

We previously made the unexpected finding that platelet depletion (acute thrombocytopenia) in RIP1-Tag2 (RT2) mice with late-stage pancreatic neuroendocrine carcinoma induced a dramatic loss of NG2-positive ($NG2^+$) pericytes from the tumor vessels (16). Platelet depletion also resulted in significantly impaired perfusion of tumor blood vessels and a concomitant reduction in tumor cell proliferation. Indeed, platelets have been described as "guardians of the tumor vasculature" (17), because acute thrombocytopenia induces hemorrhage in tumors (18). Similar observations have also been made in other situations involving active remodeling of the vasculature (19). The mechanism underlying this role of platelets in the tumor vasculature is not fully understood, but was reported to be independent of the capacity of platelets to aggregate. Instead, it was concluded that a secreted factor was responsible for the protective effect exerted by platelets on the tumor vessels (18). Whether loss of pericytes is a contributing factor to the tumor vascular damage induced by acute thrombocytopenia is unknown.

By which mechanism could platelets promote pericyte recruitment to tumor vessels? Platelets represent a major source of PDGFB, which is stored in their α-granules and released upon activation. In the tumor microenvironment, platelets are constantly activated because of aberrant expression of tissue factor (TF), leading to generation of thrombin, a potent platelet activator (20). In addition, the discontinuous tumor endothelium exposing subendothelial compartments, containing for example collagen, is another strong activation signal for

[1]Department of Medical Biochemistry and Microbiology, Science for Life Laboratory, Uppsala University, Biomedical Center, Uppsala, Sweden. [2]Wihuri Research Institute and Translational Cancer Medicine Research Program, Biomedicum Helsinki, 00014 University of Helsinki, Yliopistonkatu, Helsinki, Finland. [3]Department of Biotechnology, Govt. Arts College, Thiruvananthapuram, India. [4]Department of Immunology, Genetics and Pathology, Uppsala University, Rudbeck Laboratory, Uppsala, Sweden. [5]Department of Medical Sciences, Uppsala University, Uppsala, Sweden. [6]ICMC (Integrated Cardio Metabolic Centre), Karolinska Institutet, Novum, Blickagången 6, Huddinge, Sweden.

Note: Supplementary data for this article are available at Cancer Research Online (http://cancerres.aacrjournals.org/).

Corresponding Author: Anna-Karin Olsson, Uppsala University, Biomedical Center, Box 582, BMC, Husargatan 3, Uppsala 75123, Sweden. Phone: 461-8471-4399; Fax: 461-8471-4673; E-mail: anna-karin.olsson@imbim.uu.se

Cancer Res 2020;80:3345–58

doi: 10.1158/0008-5472.CAN-19-3533

platelets (21). As described above, PDGFB expressed by the endothelium is critical for proper pericyte recruitment to blood vessels (8, 9). However, in a tumor, there is an ongoing extensive vascular remodeling and additional sources of PDGFB could potentially contribute to maintain a sufficient level of pericyte coverage. Platelets activated in the tumor vasculature could provide such an additional source of PDGFB. To test this hypothesis, we generated genetically modified mice that lack PDGFB specifically in the megakaryocyte/platelet lineage using the Cre/loxP system. These mice were further crossed to the transgenic RT2 mouse, which develops orthotopic pancreatic neuroendocrine tumors. Using this model, as well as two additional transplanted models for tumor growth, we address the consequences of lacking PDGFB in platelets for the vascular phenotype and malignant progression.

Materials and Methods

Mice

Animal work was approved by the local ethics committee (5.8.18-09777/2018) and performed according to the United Kingdom Coordinating Committee on Cancer Research guidelines for the welfare of animals in experimental neoplasia (22). Mice of different genotypes were generated and compared as littermates. Sample size (n) is given in each figure legend. Analyses were performed in a blinded fashion where relevant, including quantification of immunohistologic stainings, the angiogenic switch, and measurement of tumor volumes. Randomization was not applicable, as no treatments were performed. All mice used in the study were on C57BL/6 background. To deplete PDGFB specifically in platelets, *Pf4-Cre* mice (C57BL/6-Tg(Pf4-cre) Q3Rsko, The Jackson Laboratory; ref. 23) were crossed with $Pdgfb^{fl/wt}$ mice (B6.129P2-Pdgfb^{tm2Cbet}, The Jackson Laboratory; ref. 8) to generate *Pf4-Cre;*$Pdgfb^{fl/wt}$ mice, which were then bred with $Pdgfb^{fl/wt}$ mice again to acquire the *Pf4-Cre;*$Pdgfb^{fl/fl}$ mice. To obtain RT2-positive (01XD5, NCI-MMHCC) mice that lack PDGFB in platelets, $Pdgfb^{fl/fl}$ mice were crossed with RT2 mice to generate *RT2;*$Pdgfb^{fl/wt}$ mice, which were bred with *Pf4-Cre;*$Pdgfb^{fl/wt}$ mice to acquire *RT2;Pf4-Cre;*$Pdgfb^{fl/fl}$ mice. DNA extracted from tail biopsies was used for genotyping by PCR. Primers used for PCR are listed in the online Supplementary Materials and Methods. From 10 weeks of age, RT2-positive mice received drinking water supplied with 10% sucrose, to relieve hypoglycemia.

Antibodies and primer sequences

A complete list of antibodies used in this study, including concentrations, as well as primer sequences used for genotyping or qPCR, are included in the online Supplementary Materials and Methods.

Platelet depletion

Mice were depleted from platelets by an intraperitoneal injection with an antibody against Gp1bα (R300, Emfret Analytics). Platelet depletion was performed from 11 weeks of age with repeated injections every third day with a total six injections per mouse. Antibody dosage was 4 μg antibody/g body weight at first injection and 2 μg antibody/g body weight at subsequent injections.

Immunostainings

Cryosections (5 μm) fixed in ice-cold methanol were used for all immunostainings if not specified. Fixation with ice-cold acetone was used for CD41 stainings of embryonic livers and for PDGFRβ stainings. For megakaryocyte staining (anti-CD41) of embryonic livers, IHC was performed using a TSA-Biotin Kit, according to the manufacturer's instructions (NEL700A001KT, Perkin Elmer). Slides were developed using 3-amino-9-ethylcarbazole solution, counterstained with hemalum solution, and mounted with Aquatex (VWR International). For megakaryocyte stainings (anti-CD41) of bone marrow, tibias were dissected, fixed in 3% paraformaldehyde (PFA) for 24 hours, and put in 10% EDTA/PBS solution (pH 7.2) for 14 days to decalcify the bones. The tissue was then embedded in OCT and sectioned.

Quantification of pericyte coverage, vascular leakage, and perivascular platelets

Pericyte coverage was evaluated by quantification of the NG2/PDGFRβ/desmin-positive area and calculation of the ratio to the CD31-positive area (NG2 or PDGFRβ or desmin/CD31). The amount of extravasated fibrinogen (vascular leakage) was evaluated by quantification of the fibrinogen-positive area and subtraction of the CD31-positive area. Perivascular platelets were evaluated by quantification of the CD41-positive area within approximately 7 μm distance from the CD31-positive area.

ELISA

Blood was sampled from the tail vein, left to coagulate overnight at 4°C, and centrifuged at 1,500 × g for 5 minutes to collect serum. ELISA was performed according to the instruction of the Quantikine ELISA Kit for mouse/rat PDGF-BB (MBB00, R&D Systems) and mouse/rat TGFβ1 (MB100B, R&D Systems). For PDGFB ELISA, mouse serum was diluted 1:10 in Calibrator Diluent RD6-3 supplied with the kit. For TGFβ1 ELISA, mouse serum was diluted 1:150 in Calibrator Diluent RD5-53 supplied with the kit.

Endothelial cell sorting and qPCR

Mice were anesthetized by intraperitoneal injection of 2% avertin. Lungs were dissected and digested with 5 mg/mL Collagenase II and 50 μg/mL DNase I (both from Sigma-Aldrich) in DMEM for 40 minutes at 37°C in a shaking incubator. Lung lysates were passed through a 70-μm cell strainer and erythrocyte lysis was performed on ice. The samples were blocked with Fc block (101302, BioLegend) and stained with anti-CD31-PE (553373, BD Biosciences) and anti-CD45-APC (103112, BioLegend) for 40 minutes. After washing with FACS sorting buffer (2% BSA/1 mmol/L EDTA/PBS), samples were stained with DAPI for live/dead discrimination. Endothelial cells ($CD45^{-}CD31^{+}$) were sorted using a FACSaria III (BD Biosciences), collected in PBS, centrifuged, and RNA was extracted using the NucleoSpin RNA Plus Kit (740984, Macherey-Nagel). cDNA was generated using the iScript cDNA Synthesis Kit (1708891, Bio-Rad) and KAPA SYBR FAST qPCR Kit (KK4608, Kapa Biosystems) was used for the PCR reaction. Primers are listed in online Supplementary Materials and Methods.

qPCR array

Lungs from C57BL/6 mice were cut into small pieces using a scalpel and added into a C-Tube (130-096-334, Miltenyi Biotec) with DMEM supplemented with collagenase (7 mg/mL, LS004176, Worthington) and DNase (1 μg/mL, D4513, MilliporeSigma). Lungs were then mechanically dissociated on a MACS Octo Dissociator (Miltenyi Biotec) using the m_LDK_1 program. Erythrocytes were lysed using Red Blood Cell Removal Solution (130-094-183, Miltenyi Biotec). Endothelial cell isolation was performed following the "isolation of endothelial cells from mouse lung" protocol from Miltenyi Biotec, using Mouse CD45 Microbeads (130-110-618, Miltenyi Biotec) for depletion of immune cells and Mouse CD31 Microbeads (130-097-418, Miltenyi Biotec) for CD31 enrichment, following the instructions

provided by the manufacturer. RNA was extracted using the RNeasy Plus Micro Kit (74004, Qiagen). Eighty-four genes related to endothelial cell biology were analyzed with the RT^2 Profiler PCR Array for Mouse Endothelial Cell Biology (PAMM-015Z, Qiagen), using a Bio-Rad CFX96 instrument, according to instructions from the manufacturer. Normalization was performed against β2-microglobulin. Analyzed genes are listed in the online Supplementary Data (EC qPCR array).

Platelet counts

Mice were anesthetized by intraperitoneal injection of 2% avertin. Blood was drawn by cardiac puncture and ACD buffer (38 mmol/L citric acid; 75 mmol/L trisodium citrate; and 100 mmol/L dextrose) was added to 40% of the total blood volume for anticoagulation. Platelet counts were analyzed using a Sysmex XP-300 Hematology Analyzer (Sysmex).

Platelet activation

Mice were anesthetized by intraperitoneal injection of 2% avertin. Blood was drawn by cardiac puncture with ACD buffer as described under Platelet counts. ADP (10 μmol/L, A2754, MilliporeSigma) or 0.01 U/mL thrombin (HCT-0020, Haematologic Technologies) was used to activate platelets. Degree of platelet activation was measured as surface expression of GpIIb/IIIa (M023-2, Emfret Analytics) and P-selectin (M130-2, Emfret Analytics), detected by flow cytometry (FC500, Beckman Coulter) as described previously (24).

FITC-lectin perfusion

Mice were anesthetized by intraperitoneal injection of 2% avertin, and FITC-lectin (Lycopersicon Esculentum, FL-1171, Vector Laboratories) was administered by retro-orbital injection of 150 μL solution (0.5 mg/mL) and allowed to circulate for 2 minutes, before perfusion with 10 mL of 1× PBS (pH 7.4) and 10 mL of 2% PFA. Tumors and organs were stored in 30% sucrose at 4°C overnight, frozen in OCT Cryomount (45830, Histolab), and stored at −70°C. Cryosections (5 μm) of tumors and organs were stained with anti-CD31 to visualize the total vessel area. FITC-lectin perfusion was evaluated by quantifying the ratio of FITC-lectin/CD31-positive area.

Analysis of angiogenic islets and tumor volume in the RT2 model

Mice were anesthetized by intraperitoneal injection of 2% avertin and perfused with 10 mL of 1× PBS (pH 7.4) and 10 mL of 2% PFA. The pancreas was dissected from 7-week-old mice and angiogenic islets were counted in a stereo dissection microscope at ×16 magnification. Tumors were isolated from the dissected pancreas of 14-week-old mice and tumor volumes were calculated [$(\pi/6) \times \text{width}^2 \times \text{length}$].

MC38 model

The MC38 mouse colon carcinoma cells were obtained through Prof. Kristofer Rubin (Uppsala University, Uppsala, Sweden) and cultured in DMEM Glutamax (31966021, Invitrogen) containing 10% FBS (Euroclone) and 1% penicillin/streptomycin (SVA, Uppsala, Sweden) at 37°C and 5% CO_2. The cells went through maximum five passages after thawing and were screened for *Mycoplasma* using PCR (last date for testing: March 3, 2020; ref. 25). The cell line was not authenticated in our laboratory. MC38 cells (0.5×10^6) in 100 μL PBS were injected subcutaneously in RT2-negative wild-type (WT) and pl-PDGFB–knockout (KO) mice and allowed to engraft for 18 days. Before sacrifice, mice were FITC-lectin perfused as described above. Tumors were dissected and frozen in OCT Cryomount (45830, Histolab).

HCmel12 model

HCmel12 melanoma cells were obtained from Prof. Thomas Tueting (University Hospital Magdeburg, Magdeburg, Germany; ref. 26). Cells were cultured in RPMI1640 medium (R0883, Invitrogen) containing 10% FBS (Euroclone), 1% penicillin/streptomycin (SVA), and 1% L-glutamine at 37°C and 5% CO_2, and regularly screened for *Mycoplasma* by LONZA MycoAlert Mycoplasma Detection Kit (LT07-701; last date for testing: May 15, 2019). The cell line was not authenticated in our laboratory. HCmel12 cells (0.5×10^6 cells in 100 μL PBS) were injected subcutaneously into RT2-negative WT and pl-PDGFB–KO mice, and allowed to engraft for 24 days. Mice were sacrificed by cervical dislocation, and lungs were dissected and frozen in OCT Cryomount (45830, Histolab).

Analysis of spontaneous metastases

Spontaneous liver metastasis was analyzed in RT2 mice and spontaneous lung metastasis was analyzed in mice with subcutaneously injected HCmel12 melanoma cells. RT2 mice (14 weeks of age) were anesthetized with 2% avertin and perfused with 10 mL of 1× PBS and 10 mL 2% PFA. Mice with HCmel12 tumors were sacrificed by cervical dislocation 24 days after tumor cell injection. Tissues were frozen in OCT Cryomount (45830, Histolab) and metastases were quantified in 5 μm cryosections from livers (RT2 mice) and lungs (HCmel12 mice) stained with hematoxylin and eosin (H&E; 01820 and 01650, Histolab). Tissue sections from four different levels of the organ were analyzed with 200 μm between each level. The average number of metastases per level was calculated for each individual mouse.

Circulating tumor cells

Circulating tumor cells (CTC) were quantified in blood from RT2 mice, by qPCR for T-antigen and insulin (primer sequences in online Supplementary Materials and Methods). Blood was drawn by heart puncture (anticoagulated with ACD buffer as described under platelet counts) and mixed with RNA Later Solution (AM7020, Invitrogen). RNA was isolated from the samples using the RiboPure Blood Kit (Life Technologies/Ambion). The iScript cDNA Synthesis Kit (1708891, Bio-Rad) and KAPA SYBR FAST qPCR Kit (KK4608, Kapa Biosystems) were used for cDNA synthesis and PCR reaction.

B16 tail vein injections

B16 melanoma cells (ATCC) were cultured in DMEM Glutamax (31966021, Invitrogen) containing 10% FBS (Euroclone) and 1% penicillin/streptomycin (SVA) at 37°C and 5% CO_2. The cells were not authenticated after purchase, but retained melanin production and were regularly tested negative for *Mycoplasma* using PCR (last date for testing: March 3, 2020; ref. 25). B16 cells (0.5×10^6 cells in 100 μL PBS) were injected in WT and pl-PDGFB–KO mice via the tail vein. Mice were sacrificed after 14 days and lungs were dissected. Metastatic analysis was performed by counting visible metastatic foci on the surface of the lung lobes.

Proximity ligation assay

Proximity ligation assay (PLA) was performed using the Duolink PLA Products (MilliporeSigma) according to a standard protocol at the PLA Proteomic Facility SciLifeLab (Uppsala University, Uppsala, Sweden). Briefly, 3.7% PFA-fixed tumor cryosections were permeabilized with 0.5% Triton-X 100 in PBS and blocked at 37°C during 1 hour in Duolink blocking solution with 200 μg/mL donkey anti-mouse IgG (715-005-150, Jackson ImmunoResearch). Cryosections were incubated at 4°C overnight with goat anti-mouse PDGFRβ and anti-mouse pY-100 primary antibodies, washed for 5 minutes for three

times with TBST, followed by 1 hour incubation with Duolink PLA Secondary Probes (MilliporeSigma), anti-mouse PLUS (DUO92001), and anti-goat MINUS (DUO92006) at 37°C. Cryosections were washed in TBST and incubated for 30 minutes at 37°C in ligation solution. The PLA signal was amplified by rolling-circle amplification by using phi29 polymerase (27). Nuclei were detected by Hoechst. Cryosection slides were mounted for microscopy analysis by using SlowFade Gold Antifade Reagent (S36936, Invitrogen). Single primary antibody with PLA probes and PLA probes without primary antibodies were routinely included as negative controls. The phospho-PDGFRβ signaling was evaluated by quantifying the PLA signal–positive area. Costaining for NG2 was performed by adding the rabbit anti-mouse NG2 antibody together with the PLA primary antibodies and the anti-rabbit Alexa488 secondary together with the Duolink secondary probes.

Image analysis

Imaging of tissue sections stained by immunofluorescence or H&E was done using a Nikon Eclipse 90i Microscope and the NIS Elements 3.2 software. Images were analyzed using the ImageJ 1.45s Software (NIH, Bethesda, MD). Chromogenic slides were imaged with Leica DM LB Bright-Field Microscope and Olympus Digital Camera. Studio Lite software was used for image acquisition. Images of embryos were obtained with a dissecting microscope (model S6; Leica) connected to a Sony camera with Image-Pro version 3.0.1 software.

Statistical analysis

All statistical analyses in this study were performed using the nonparametric two-tailed Mann–Whitney test, because sample sizes are small ($n < 50$) and, therefore, difficult to test for normality. In this study, n always represents individual samples. *, $P \le 0.05$; **, $P \le 0.01$; ***, $P \le 0.001$; ****, $P < 0.0001$. Exact P values are given in the respective figure legend.

Results

Platelet depletion induces pericyte loss in tumor vessels

We have previously reported that platelet depletion in RT2 mice with pancreatic neuroendocrine carcinomas resulted in an almost complete loss of $NG2^{+}$ pericytes (16), and we first confirmed this finding (**Fig. 1A**). Because pericytes may show plasticity in marker expression, we addressed whether other pericyte markers were also lost. Immunostaining for the pericyte markers PDGFRβ (**Fig. 1B**) and desmin (**Fig. 1C**) in tumor tissue from control or platelet-depleted RT2 mice revealed that cells expressing these pericyte markers were also significantly reduced in tumor vessels after induction of thrombocytopenia. These results suggest that the abundance of differentiated pericytes in pancreatic tumors is indeed reduced following platelet depletion. This finding might reflect a failure of corecruitment of pericyte progenitors to newly formed tumor vessels, or that newly recruited pericytes die or dedifferentiate. Irrespective of these alternative mechanisms, RT2 tumor vessels fail to acquire a coat of differentiated pericytes after platelet depletion. In agreement with previous findings (18), we also detected increased leakage from tumor vessels after platelet depletion (**Fig. 1D**).

Generation of mice with PDGFB-deficient platelets

Activated platelets secrete PDGFB, a factor also expressed by endothelial cells and known to be essential for pericyte recruitment during developmental angiogenesis (6, 8). To investigate whether platelet-derived PDGFB mediates recruitment of pericytes to tumor vessels, we generated a conditional knockout of PDGFB in megakaryocytes and, consequently, platelets. Mice expressing the Cre-recombinase under the platelet factor 4 (PF4) promoter (*Pf4-Cre*), specific for the megakaryocyte lineage (23), were crossbred to $Pdgfb^{fl/fl}$ mice, containing loxP sites flanking exon 4 in the *Pdgfb* gene (8). Theoretically, this should result in functional inactivation of floxed *Pdgfb* alleles in all megakaryocytes and hence platelets (**Fig. 2A**). Different genotypes were detected with specific primers as described in Materials and Methods and generated PCR products of distinct sizes as illustrated in **Fig. 2B**. Mice lacking PDGFB in the megakaryocyte lineage (*Pf4-Cre;*$Pdgfb^{fl/fl}$) were viable and fertile. It was previously demonstrated that the floxed *Pdgfb* allele is functional (8), therefore, mice with genotypes $Pdgfb^{fl/fl}$, $Pdgfb^{fl/wt}$, $Pdgfb^{wt/wt}$ *or Pf4-Cre* served as PDGFB WT controls.

Macroscopic examination of *Pf4-Cre;*$Pdgfb^{fl/wt}$ and *Pf4-Cre;*$Pdgfb^{fl/fl}$ embryos at different gestational stages (E14.5, E15.5, and E17.5) revealed no abnormal phenotype (Supplementary Fig. S1A–S1C). Also the number of viable *Pf4-Cre;*$Pdgfb^{fl/fl}$ embryos were the same as the expected (Supplementary Table S1). *Pdgfb* mutants displayed the same number and distribution pattern of CD41-positive megakaryocytes (platelet precursors) in embryonic livers, an important site of hematopoiesis during development (Supplementary Fig. S1D–S1F). Equal number of bone marrow megakaryocytes were also detected by immunostaining for CD41 in tibias from adult mice (Supplementary Fig. S1G–S1I). These data suggest that platelet-specific knockout of PDGFB (pl-PDGFB KO) does not influence the number of megakaryocytes, either during development or in the adult mouse. Importantly, platelet counts in pl-PDGFB–KO and WT mice were similar (Supplementary Fig. S2A), as was the proportion of platelets among other cell types in peripheral blood (Supplementary Fig. S2B).

To address whether the Cre-loxP recombination in megakaryocytes was sufficiently efficient to remove PDGFB from platelet releasates, we analyzed PDGFB protein levels in serum samples from mice with different genotypes using ELISA. *Pf4-Cre;*$Pdgfb^{fl/fl}$ mice had undetectable levels of PDGFB in serum in contrast to *Pf4-Cre;*$Pdgfb^{wt/wt}$ and *Pf4-Cre;*$Pdgfb^{fl/wt}$, where the *fl/wt* mice displayed approximately half of the serum PDGFB concentration (3.2 ng/mL) compared with the *wt/wt* mice (5.3 ng/mL; **Fig. 2C**). These data demonstrate a functional Cre-loxP recombination, and hence removal of PDGFB from platelet granules. Interestingly, this result also shows that all detectable PDGFB in mouse serum is derived from platelets. To confirm that the conditional knockout did not affect endothelial PDGFB expression, $CD31^{+}$ cells extracted by FACS from lungs derived from WT or pl-PDGFB–KO mice were analyzed for expression of PDGFB by qPCR. No difference in endothelial PDGFB expression was detected between WT and pl-PDGFB–KO mice (**Fig. 2D**).

To address whether platelet-specific deletion of PDGFB could have secondary effects on the vasculature, we analyzed the expression of 84 distinct genes related to endothelial cell biology by qPCR arrays in lung endothelial cells sorted from pl-PDGFB–KO and WT mice. For seven of the 84 genes, there was no detectable signal in one or more of the samples. For the remaining 77 genes, all samples generated a detectable signal and the analysis showed that there were no statistically significant differences in gene expression between pl-PDGFB–KO and WT mice (see online Supplementary Data: EC qPCR array).

Lack of PDGFB does not affect platelet activation

To make sure that platelet activation was not compromised by the lack of PDGFB, we monitored P-selectin and fibrinogen receptor expression on the platelet surface after stimulation of whole blood with thrombin and ADP, respectively, using FACS. Platelets from

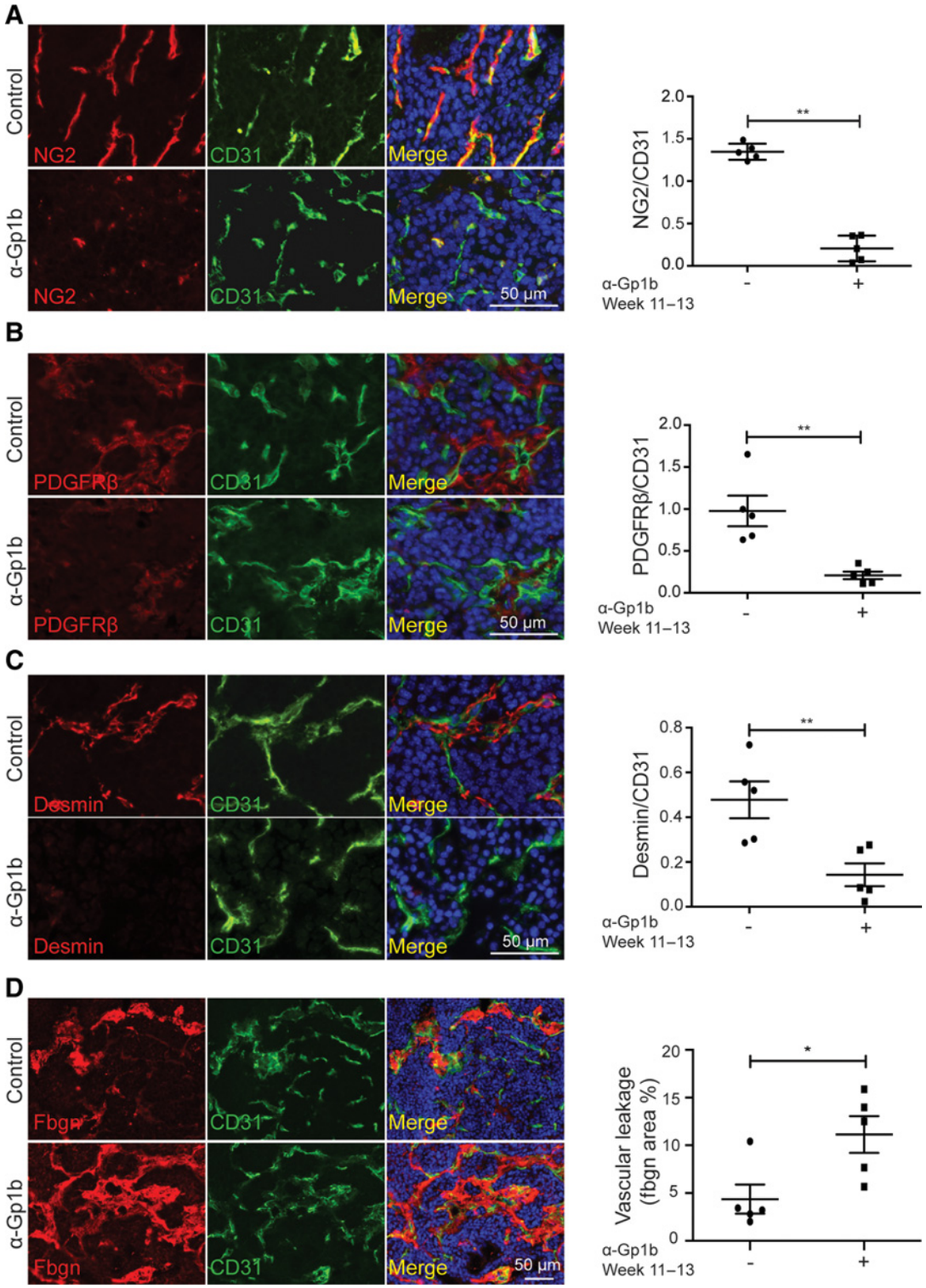

Figure 1.

Pericyte coverage is decreased in the tumor vasculature after platelet depletion. Immunostaining for pericyte markers NG2 ($n = 5$/group; $P = 0.0079$; **A**), PDGFRβ ($n = 5$/group; $P = 0.0079$; **B**), and desmin ($n = 5$/group; $P = 0.0079$; **C**) and the amount of extravasated fibrinogen (fbgn) as a read out for vascular leakage ($n = 5$/group; $P = 0.0317$; **D**) in tumor tissue from platelet-depleted RT2 mice. Platelet depletion was performed using an anti-Gp1b antibody during 2 weeks (RT2 age week 11–13). Error bars, SEM. *, $P \leq 0.05$; **, $P \leq 0.01$.

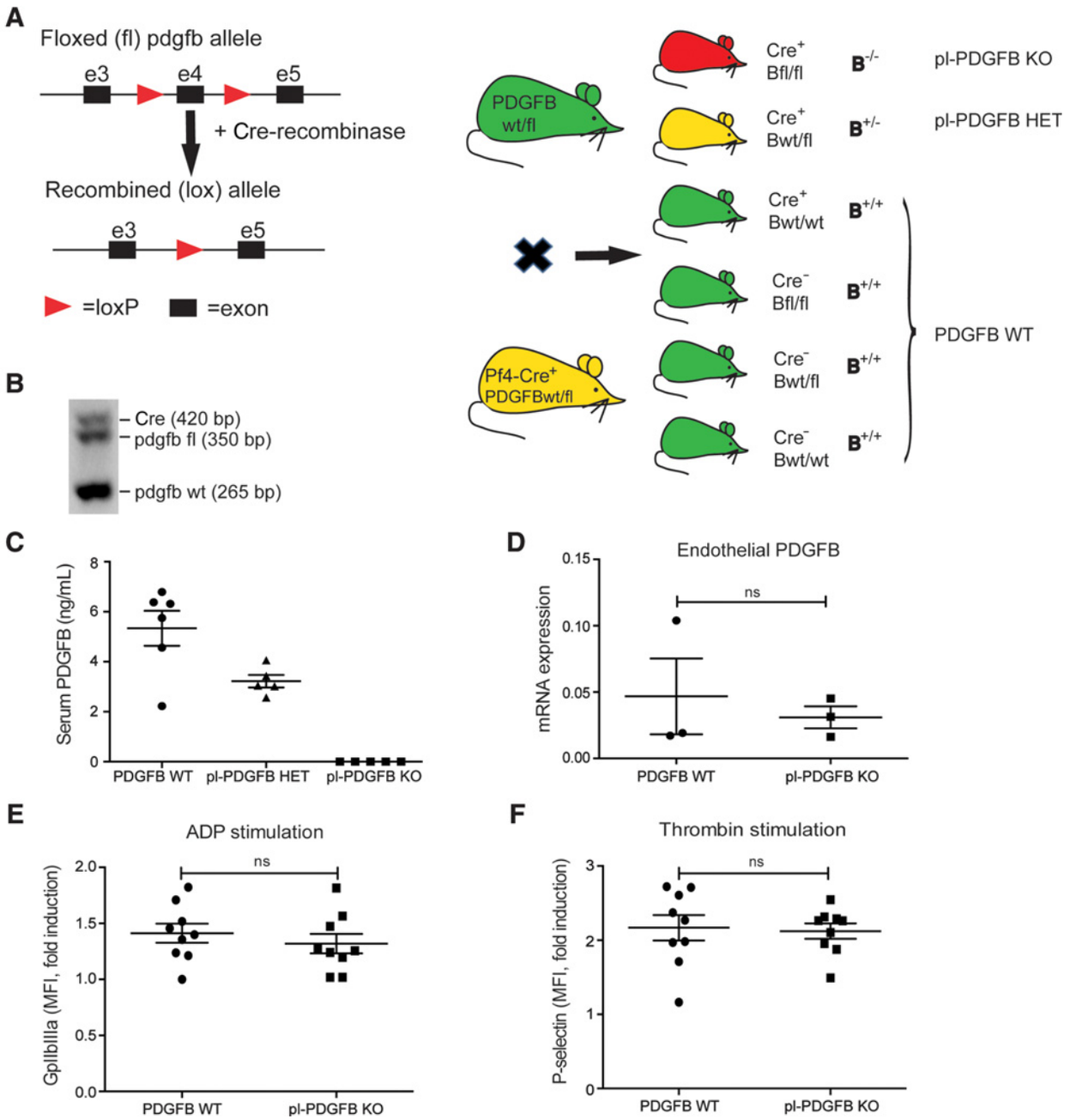

Figure 2.

Generation of mice lacking PDGFB in platelets. **A,** Mice lacking PDGFB in the platelet/megakaryocyte lineage were generated using the Cre-loxP recombination system, with Cre expressed under the PF4 promoter. Green mice are PDGFB WT, yellow mice are pl-PDGFB heterozygotes (pl-PDGFB HET), and red mice are pl-PDGFB KO. **B,** Genotyping was performed for the WT and floxed (fl) *Pdgfb* alleles, as well as for *Cre* and generated PCR products of sizes 265, 350, and 420 bp, respectively. **C,** PDGFB concentration in serum from WT ($n = 6$), pl-PDGFB HET ($n = 5$), and pl-PDGFB-KO ($n = 5$) mice was determined using ELISA. **D,** PDGFB mRNA expression (relative to the housekeeping gene β2-microglobulin) in lung endothelial cells sorted by FACS from WT and pl-PDGFB–KO mice ($n = 3$/group; $P > 0.9999$). **E** and **F,** Platelet activation in whole blood from healthy WT and pl-PDGFB–KO mice was assayed in response to ADP and thrombin. The activation was measured as expression of the fibrinogen receptor (GpIIbIIIa; $n = 9$/group; $P = 0.5457$; **E**) and P-selectin ($n = 9$/group; $P = 0.5457$; **F**) by FACS. Error bars, SEM. MFI, mean fluorescence intensity; ns, not significant.

Pf4-Cre;Pdgfb$^{fl/fl}$ mice responded equally well to the activation stimulus as platelets from control mice with intact PDGFB levels in their platelets (**Fig. 2E** and **F**), demonstrating that lack of PDGFB does not affect the capacity of platelets to become activated.

Lack of platelet-derived PDGFB does not affect the vascular phenotype in kidney tissue

To address whether genetic ablation of PDGFB in platelets has functional consequences for healthy vasculature, we analyzed

perfusion, leakage, and pericyte coverage in kidney tissue from mice with or without PDGFB in their platelets (**Fig. 3**). Specifically, we selected kidney glomeruli for analysis because previous work has shown this structure to be particularly sensitive to the genetic loss of *Pdgfb* or its receptor-encoding gene *Pdgfrb* (5, 9, 10, 28). We could not find any differences between the genotypes with respect to vascular perfusion (**Fig. 3A**), fibrinogen extravasation (**Fig. 3B**), or the amount of $NG2^+$ vessels (**Fig. 3C**). We, therefore, conclude that platelet-derived PDGFB is dispensable for pericyte recruitment and does not affect vascular function in a healthy tissue such as the kidney.

Lack of platelet-derived PDGFB does not affect the angiogenic switch or total tumor burden in mice with pancreatic neuroendocrine carcinoma

Mice with *Pf4-Cre* and floxed *Pdgfb* alleles were cross-bred with the RT2 mouse, which develops pancreatic neuroendocrine carcinoma through a series of well-defined steps (Supplementary Fig. S3A; ref. 29). From this breeding, a number of different genotypes were generated, as illustrated in Supplementary Fig S3B. In addition to the genotypes described in **Fig. 2**, transmission of the oncogenic RT2 allele was assayed by PCR, generating a 449-bp fragment. Because of the similarities in size between the RT2 and Cre PCR products, the presence of Cre was analyzed separately (Supplementary Fig. S3C).

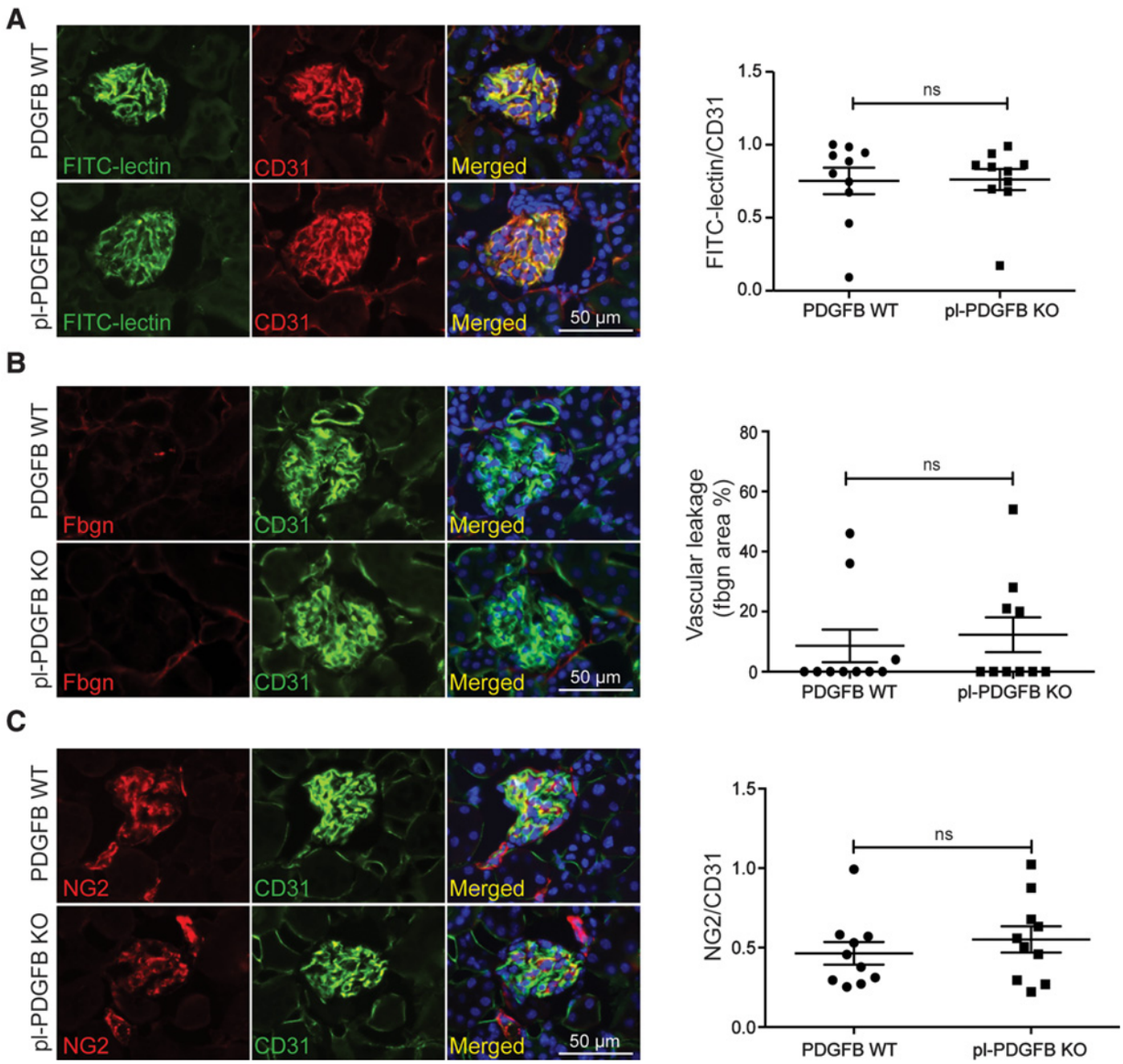

Figure 3.
Vascular phenotype in healthy kidney tissue is not affected by platelet-specific PDGFB deficiency. Sections of kidney tissue from FITC-lectin perfused WT, and pl-PDGFB–KO RT2-negative mice were immunostained for CD31 and analyzed for the proportion of FITC-lectin perfused vessels (FITC/CD31 ratio; $n = 10$/group; $P = 0.8534$; **A**), the amount of extravasated fibrinogen (fbgn) as a read out for vascular leakage ($n = 10$/group; $P = 0.7214$; **B**), and the extent of $NG2^+$ pericyte coverage ($n = 10$/group; $P = 0.4813$; **C**). Error bars, SEM. ns, not significant.

A proportion of the hyperplastic and dysplastic lesions that develop in the insulin-producing islets of Langerhans in the pancreas of RT2 mice undergo an angiogenic switch with onset at around 7–8 weeks of age (29, 30). This means that the islets initiate active angiogenesis, which is largely governed by increasing hypoxia and elevated levels of VEGFA (31). The angiogenic islets can be detected under a microscope by their red color in the dissected pancreas. Quantification of the angiogenic switch revealed no significant difference between the two groups of mice (Supplementary Fig. S4A). The angiogenic islets subsequently develop into adenomas and ultimately carcinomas as the mice age. Analyzing the total tumor burden at week 14 of age, we could not find any difference in tumor volumes between WT and pl-PDGFB–KO mice (Supplementary Fig. S4B). However, in 8 of total 18 analyzed pl-PDGFB KO mice, the tumors were connected to blood-filled cysts of varying size, which was never observed in the WT mice (Supplementary Fig. S4C).

Immunostaining for platelets (CD41) revealed a clear increase in the number of adhering, and thus activated, platelets in tumor tissue compared with healthy kidney tissue, as expected (Supplementary Fig. S4D). No difference was detected between WT and pl-PDGFB–KO mice with respect to the amount of tumor adherent platelets, quantified either as total amount (Supplementary Fig. S4E) or platelets in close proximity to vessels (Supplementary Fig. S4D–S4F), further underscoring that there is no activation defect in platelets deficient for PDGFB.

Lack of platelet-derived PDGFB reduces pericyte coverage and tumor vascular function

To address whether genetic ablation of PDGFB in platelets affects the tumor vasculature, we analyzed perfusion, leakage, and pericyte coverage in tumor tissue from 14-week-old RT2 WT and pl-PDGFB–KO mice (**Fig. 4**). We found a significant reduction in FITC-lectin perfused tumor vessels in mice with PDGFB-deficient platelets compared with control mice (**Fig. 4A**). Moreover, there was a strong and significant increase in the amount of extravasated fibrinogen detected by immunostaining of tumor tissue from pl-PDGFB–KO mice compared with WT (**Fig. 4B**), indicating increased leakage and reduced functionality of the tumor vasculature. Immunostaining for NG2 to detect pericytes revealed a significant reduction of NG2 expression in the tumor vessels of mice that lacked PDGFB in their platelets (**Fig. 4C**). Because of putative plasticity of pericytes with respect to marker expression, we also performed immunostaining for desmin and PDGFRβ, additional pericyte markers. In agreement with the NG2 data, there was a significant reduction of vascular-associated cells with desmin (**Fig. 4D**) or PDGFRβ (**Fig. 4E**) immunoreactivity, indicating that pericyte recruitment to tumor vessels is compromised in the absence of platelet-derived PDGFB.

To determine whether the requirement of platelet-derived PDGFB for pericyte recruitment and vessel functionality is specific for the RT2 model, or whether this finding applies to other tumor types also, we performed subcutaneous injections of MC38 mouse colon carcinoma cells in RT2-negative WT and pl-PDGFB–KO mice and analyzed the vascular phenotype in established tumors (Supplementary Fig. S5). In agreement with the findings in the RT2 mice, FITC-lectin perfusion was reduced (Supplementary Fig. S5A) and fibrinogen leakage was enhanced (Supplementary Fig. S5B) in mice lacking PDGFB in their platelets. Moreover, pericyte coverage in the MC38 tumor vasculature was reduced in mice with PDGFB-deficient platelets, as judged by immunostaining for NG2 (Supplementary Fig. S5C) and desmin (Supplementary Fig. S5D). This finding indicates that platelet-derived PDGFB may be of general importance for pericyte recruitment to tumor vessels.

PDGFRβ activation is reduced in tumors from mice with PDGFB-deficient platelets

To address whether lack of platelet-derived PDGFB affects signaling through PDGFRβ in the tumor microenvironment, PDGFRβ phosphorylation in RT2 tumors from 14-week-old WT and pl-PDGFB–KO mice was analyzed by *in situ* PLA. Positive PLA signals, indicating phosphorylated PDGFRβ, were detected in the WT individuals, but strongly reduced in tumor tissue from pl-PDGFB–KO mice (**Fig. 5A**). Coimmunostaining for NG2 to detect pericytes showed that the PLA signal was mainly located to pericytes (**Fig. 5B**). Negative controls (lacking primary or secondary antibody, or using noncomplementary PLA primers) did not generate any signal. These data support the conclusion that PDGFB derived from platelets contributes to modulation of the microenvironment in tumor tissue.

Enhanced metastasis in mice with PDGFB-deficient platelets

To address whether the compromised integrity of tumor vessels in *Pf4-Cre;Pdgfb*$^{fl/fl}$ mice affects dissemination of tumor cells, we analyzed WT ($n = 23$) and pl-PDGFB–KO ($n = 17$) RT2 mice for metastases in the liver using H&E staining. Not all RT2 mice develop metastasis during the time we are allowed to keep them because of ethical regulations. During this time, incidence of metastasis was not statistically different between WT ($n = 11/23$) and pl-PDGFB–KO ($n = 11/18$) mice. However, quantification of the number of metastases/liver section revealed a significant increase in the mice with PDGFB-deficient platelets compared with mice with intact PDGFB (**Fig. 6A**). To confirm the finding of increased spontaneous metastasis in pl-PDGFB–KO mice we used the HCmel12 melanoma model, which grows invasively in the skin when injected subcutaneously and forms spontaneous metastasis in the lung (26). Also, in this model there was a decrease in $NG2^+$ pericytes in the primary tumor vasculature of pl-PDGFB–KO mice compared with WT (Supplementary Fig. S6A). Of 22 HCmel12-injected mice/group, 9 WT and 15 pl-PDGFB–KO mice developed lung metastasis after 24 days. Quantification of the number of metastases/lung section revealed a significant increase in pl-PDGFB–KO mice (Supplementary Fig. S6B).

Analysis of CTCs in WT and pl-PDGFB–KO RT2 mice using qPCR for both T-antigen and insulin, expressed by the tumor cells, showed a significantly higher level of CTCs in pl-PDGFB–KO mice (**Fig. 6B**). To further address the mechanism behind the increased metastasis in pl-PDGFB–KO mice, we performed intravenous injections of B16 melanoma cells in WT and pl-PDGFB–KO mice. When the tumor cells entered directly into the circulation, without having to intravasate, there was no significant difference between the two genotypes with respect to the number of experimental metastases that formed in the lungs (**Fig. 6C**). Taken together, these data indicate that lack of platelet-derived PDGFB promotes metastasis by enhanced entry of tumor cells into the circulation.

Elevated hypoxia and enhanced epithelial-to-mesenchymal transition in tumors from mice with PDGFB-deficient platelets

Enhanced intravasation of tumor cells could be regulated by different forces. One possibility is that the reduced pericyte investment occurs already at an early stage during tumor progression, which destabilizes the vascular integrity and enables easier passage for tumor cells into the circulation. To address this possibility, we analyzed pericyte coverage in pancreatic islets from 7-week-old WT and

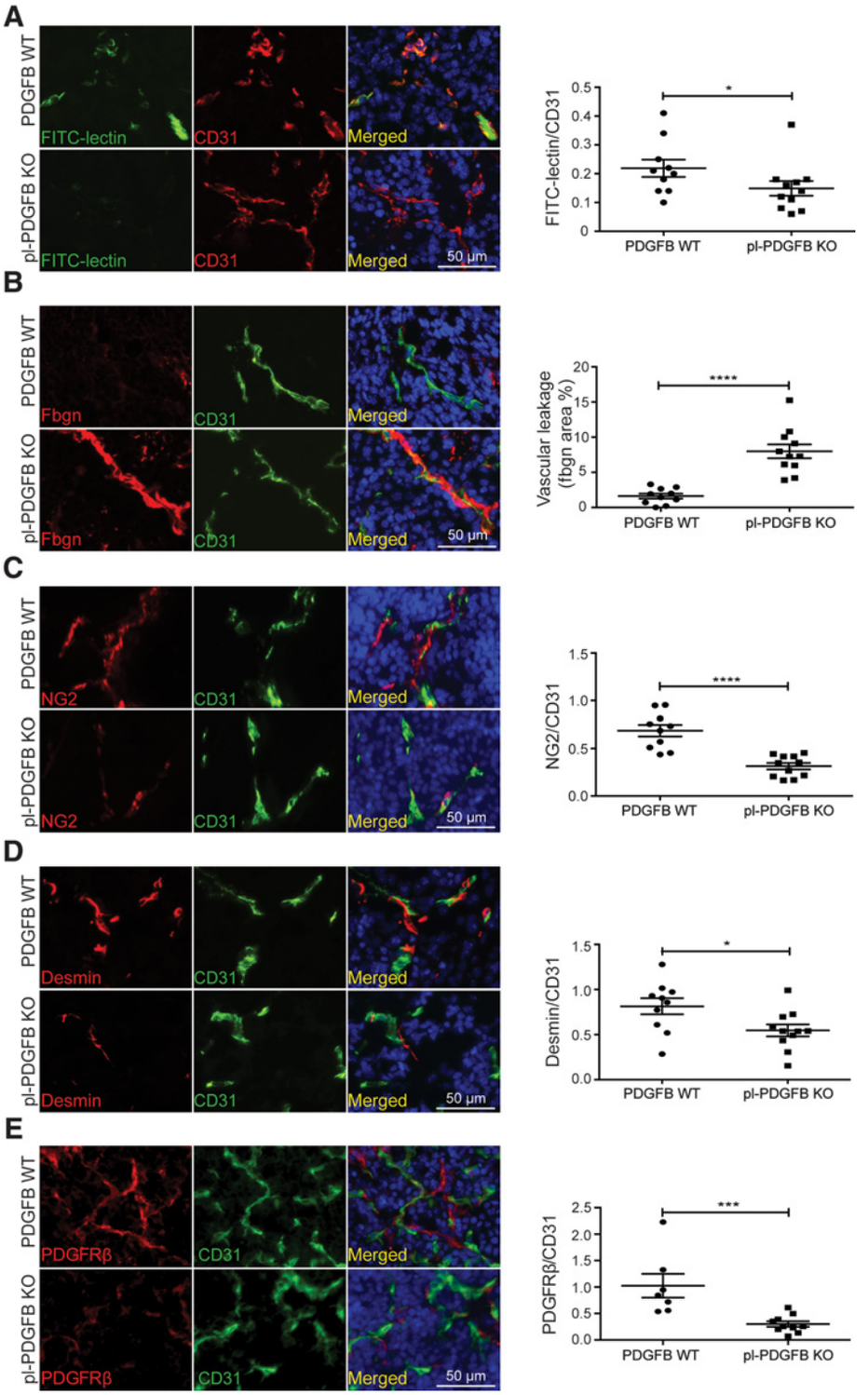

Figure 4.

Tumor vessels in mice with platelet-specific PDGFB ablation have impaired function and decreased pericyte coverage. Sections of tumor tissue from FITC-lectin perfused 14-week-old WT and pl-PDGFB–KO RT2-positive mice were immunostained for CD31 and analyzed for the proportion of FITC-lectin perfused vessels (FITC/CD31 ratio; WT, $n = 10$; KO, $n = 11$; $P = 0.0430$; **A**), the amount of extravasated fibrinogen (fbgn) as a read out for vascular leakage (WT, $n = 10$; KO, $n = 11$; $P < 0.0001$; **B**), and the extent of NG2$^+$ (WT, $n = 10$; KO, $n = 11$; $P < 0.0001$; **C**), desmin$^+$ (WT, $n = 10$; KO, $n = 11$; $P = 0.0357$; **D**), and PDGFRβ$^+$ (WT, $n = 7$; KO, $n = 10$; $P = 0.0004$; **E**) pericyte coverage. Error bars, SEM. *, $P \leq 0.05$; ***, $P \leq 0.001$; ****, $P < 0.0001$.

pl-PDGFB–KO RT2 mice. At this age, the pancreatic islets have not yet developed into carcinomas, but the angiogenic switch has been initiated (29, 30). Immunostainings for NG2 (Supplementary Fig. S7A) and desmin (Supplementary Fig. S7B) revealed a reduced pericyte coverage in the vasculature already at this early stage of tumor development. In agreement, increased vascular leakage was also detected at this stage (Supplementary Fig. S7C). Reduced vascular function can cause hypoxia, a known driver of epithelial-to-mesenchymal transition (EMT) and invasiveness (32, 33). To address the level of hypoxia in WT and pl-PDGFB–KO tumors from RT2 mice,

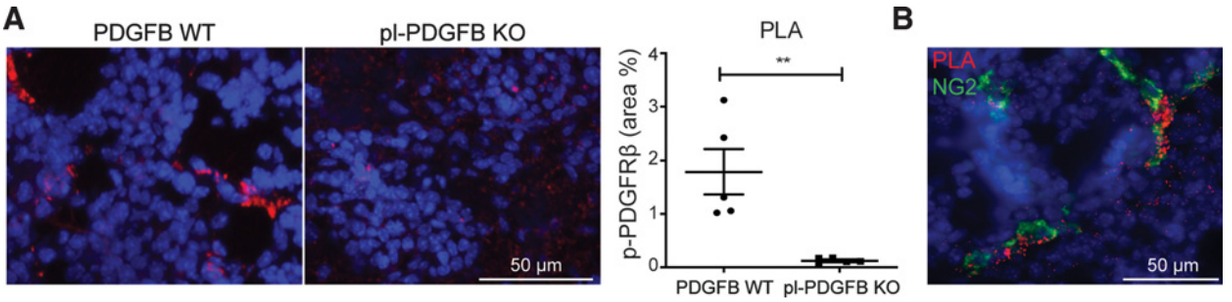

Figure 5.
Reduced PDGFRβ activation in tumors from mice with PDGFB-deficient platelets. **A,** PLA was performed on tumor tissue sections from FITC-lectin perfused 14-week-old WT and pl-PDGFB–KO RT2-positive mice (n = 5/group; P = 0.0079). The PLA-positive signal (red dots) is a read out for phospho-PDGFRβ. The graph represents the % PLA-positive area, and each dot represents one individual. **B,** Costaining for the pericyte marker NG2 in the PLA assay. Error bars, SEM. **, $P \le 0.01$.

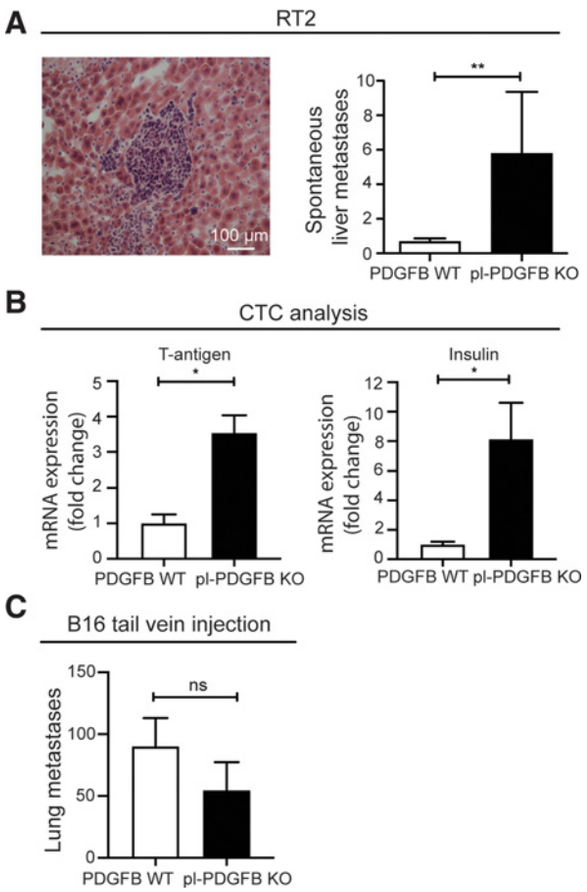

Figure 6.
Enhanced metastasis in mice lacking PDGFB in platelets. **A,** Sections of liver tissue, from four distinct levels, from 14-week-old WT and pl-PDGFB–KO RT2-positive mice were stained by H&E. The graph represents the average number of metastases/liver section in mice with metastasis (WT, n = 11; KO, n = 11; P = 0.0085). **B,** CTCs were measured in 14-week-old WT and pl-PDGFB–KO RT2-positive mice by qPCR for T-antigen and insulin using RNA extracted from blood (n = 4/group; P = 0.0286 for both). **C,** Number of lung surface metastases in WT and pl-PDGFB–KO mice injected with B16 melanoma cells via the tail vein (WT, n = 12; KO, n = 9; P = 0.1930). *, $P \le 0.05$; **, $P \le 0.01$; ns, not significant.

we analyzed expression of the hypoxia-inducible transcriptional target, HIF1α, by qPCR. As illustrated in **Fig. 7A**, we found a significant increase in HIF1α expression in tumor tissue from pl-PDGFB–KO compared with WT mice. Immunostaining for another hypoxia-inducible molecule, BNIP3, whose expression is primarily driven by HIF1α (34), revealed elevated levels in RT2 tumor tissue from mice with PDGFB-deficient platelets (**Fig. 7B**). Moreover, we found increased expression of carbonic anhydrase 9 (CA9), induced by hypoxia, in HCmel12 tumors from pl-PDGFB–KO mice (Supplementary Fig. S6C).

To address potential differences in EMT between WT and pl-PDGFB KO during early-stage tumorigenesis, expression of the epithelial markers E-cadherin and ZO-1 was analyzed by immunostaining. We found a significant reduction in the amount of E-cadherin (**Fig. 7C**) and ZO-1 (**Fig. 7D**) in the pancreatic islets from 7-week-old RT2 mice with PDGFB-deficient platelets. Moreover, expression of the mesenchymal marker vimentin was increased in tumors from pl-PDGFB–KO mice (**Fig. 7E**). Collectively, these data indicate an accelerated EMT in tumors from pl-PDGFB–KO mice.

Platelets are a major source of TGFβ and platelet-derived TGFβ was previously identified as an important driver of tumor cell EMT and metastasis (35). To confirm that the level of TGFβ in platelets was not affected in the pl-PDGFB–KO mouse, we performed an ELISA for TGFβ in serum collected from WT and pl-PDGFB–KO mice. As expected, there was no difference between the mice with respect to TGFβ levels (Supplementary Fig. S7D).

On the basis of these data, we conclude that the enhanced metastasis seen in mice with PDGFB-deficient platelets is caused by reduced tumor vessel integrity and perfusion, elevated tumor hypoxia and EMT, eventually resulting in increased intravasation of tumor cells.

Discussion

The growth factor, PDGFB, was originally isolated from platelets because of its abundance in this cell type (36), but its functional role in platelets has never been addressed using genetic models. In this study we have generated mice genetically deficient for PDGFB in megakaryocytes and hence platelets. These mice are viable and fertile with no obvious abnormalities. Pf4-Cre–mediated excision of PDGFB in platelets was confirmed by ELISA, showing undetectable levels of PDGFB in serum from *Pf4-Cre;Pdgfb*$^{fl/fl}$ mice. The absence of PDGFB in serum from *Pf4-Cre;Pdgfb*$^{fl/fl}$ mice also demonstrates that this growth factor is not freely circulating in the blood, but

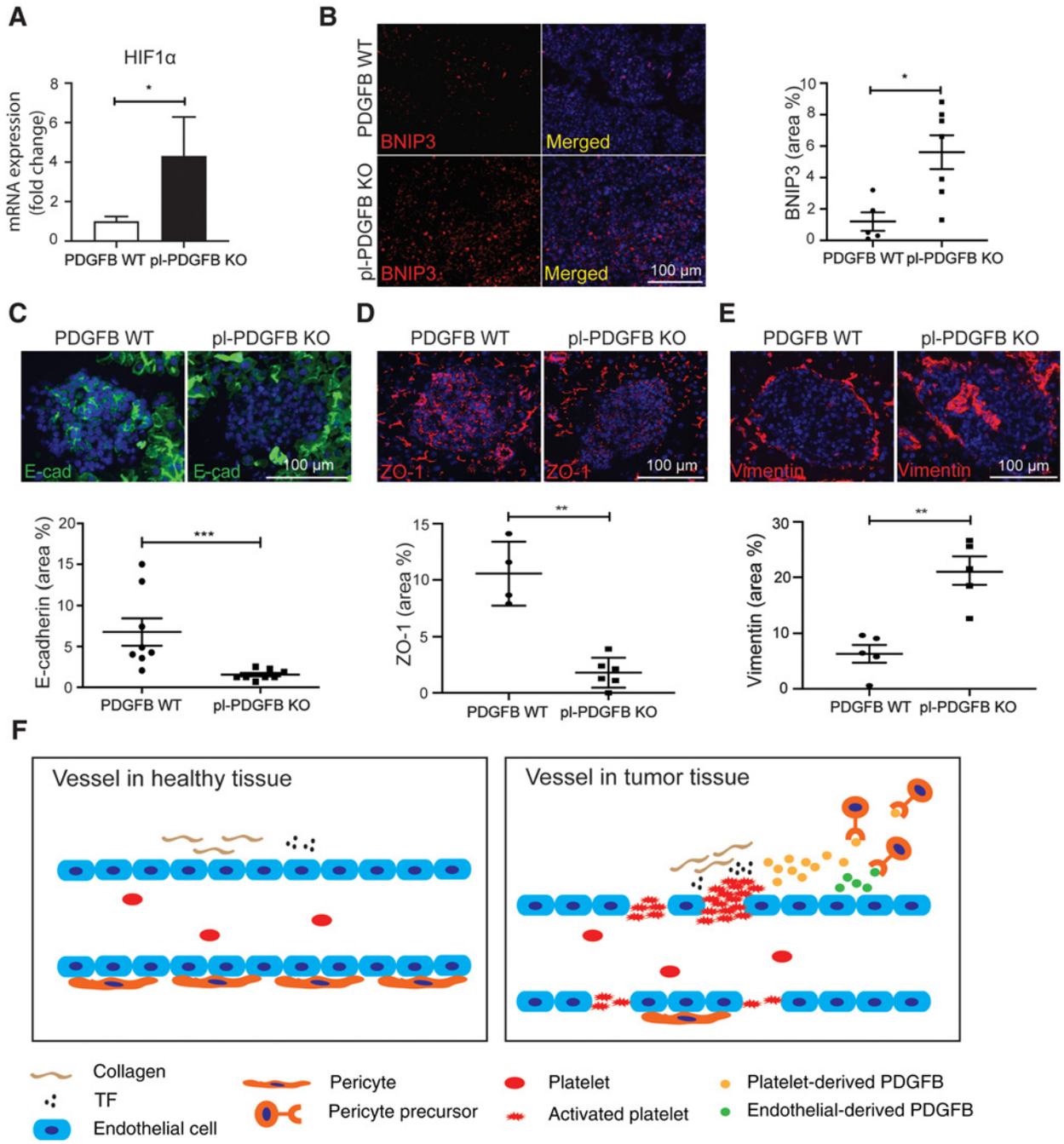

Figure 7.

Elevated hypoxia and enhanced EMT in tumors from mice with PDGFB-deficient platelets. **A,** Expression of HIF1α PDGFB mRNA (relative to the housekeeping gene β2-microglobulin) in tumor tissue from 14-week-old WT and pl-PDGFB–KO RT2-positive mice measured by qPCR (WT, $n = 4$; KO, $n = 5$; $P = 0.0159$). Immunostaining for BNIP3 (WT, $n = 5$; KO, $n = 7$; $P = 0.0177$; **B**), E-cadherin (E-cad; $n = 8$/group; $P = 0.0006$; **C**), ZO-1 (WT, $n = 4$; KO, $n = 6$; $P = 0.0095$; **D**), and vimentin ($n = 5$/group; $P = 0.0079$; **E**) in pretumorigenic tissue from 7-week-old WT and pl-PDGFB–KO RT2-positive mice. Error bars, SEM. **F,** Schematic model: in a healthy tissue, subendothelial components such as TF and collagen are not exposed to the blood and platelets are not activated, but instead stay in circulation. In a tumor, the discontinuous endothelium exposes the blood to subendothelial spaces, leading to activation and degranulation of platelets in close proximity to the vasculature. PDGFB secreted by activated platelets will, in the same way as endothelial-derived PDGFB, be retained close to the vasculature due to the heparan sulfate–binding retention-motif and thus contribute to the pericyte-recruiting gradient of PDGFB. *, $P \leq 0.05$; **, $P \leq 0.01$; ***, $P \leq 0.001$.

instead stored and released from platelets upon activation. In this way it is possible to create a high local increase in the concentration of PDGFB. The conditional deletion of PDGFB did not affect the number of bone marrow megakaryocytes, platelet counts, or the proportion of platelets in peripheral blood. This is in-line with a previous study using bone marrow chimeras, which demonstrated that lack of PDGFB expression in the hematopoietic compartment does not interfere with normal hematopoiesis (37). Importantly, platelet activation in response to ADP and thrombin, measured as expression of the fibrinogen receptor and P-selectin, was not affected by the lack of PDGFB.

Physiologically, platelets are activated upon injury because of exposure of subendothelial compartments containing TF, leading to thrombin generation, and collagen. This induces rapid arrest, conformational change, and degranulation of platelet intracellular stores. Platelet granules contain a large collection of growth factors and are a major source of VEGF and TGFβ in our bodies (38, 39). Tumors have acquired the capacity to activate platelets due to aberrant expression of TF and due to their discontinuous endothelium, exposing subendothelial spaces. As a consequence, tumors are continuously exposed to the plethora of growth factors released from platelet granules, illustrating the expression that "tumors are like wounds that do not heal" (40).

We found that tumor vessels in RT2 mice lacking platelet PDGFB displayed reduced vascular function and decreased coverage by $NG2^+$, $PDGFR\beta^+$, and $desmin^+$ mural cells, a finding that was confirmed in two additional models. These data indicate that platelet-derived PDGFB has a functional role in pericyte recruitment to the tumor vasculature. Release of PDGFB from activated platelets occurs in close proximity to the endothelium where the activating stimuli are present. Platelet-derived PDGFB should thus be present in a similar location as the endothelial-derived PDGFB, with the highest concentration retained around the endothelium (**Fig. 7F**). In the healthy noninjured tissue, arrest and activation of circulating platelets does not occur and consequently their granule content will not be released to contribute to processes in their microenvironment. This was also confirmed in our own immunostainings for platelets in healthy kidney compared with tumor tissue. In agreement, we found no difference between mice with intact or PDGFB-deficient platelets with respect to pericyte coverage or vascular function in kidney tissue from healthy mice.

Despite the reduced pericyte coverage in tumors from mice with PDGFB-deficient platelets, we did not observe any difference in tumor volumes between the genotypes in any of the three tumor models analyzed (RT2, MC38, and HCmel12). Interestingly, it has been demonstrated that blood vessels in healthy tissue can lose up to 50% of their pericytes and still retain a normal morphology (8). Even more severe pericyte deficiency is compatible with life, but this generates an abnormal vasculature both with respect to anatomy and function (8, 10). We did, indeed, detect a significant reduction in tumor vascular function in pl-PDGFB–KO mice. In addition, almost 50% of the analyzed tumors from RT2 mice with PDGFB-deficient platelets presented with blood-filled vacuoles, indicating the existence of an abnormal vascular phenotype in these mice. Previous studies of the effect of reduced pericyte coverage in tumor vasculature have been performed using the PDGFB retention motif–mutant ($Pdgfb^{ret/ret}$) mice, which display a systemic pericyte deficiency (10). In agreement with our findings, increased hemorrhage was detected in T241 fibrosarcoma subcutaneously implanted in $Pdgfb^{ret/ret}$ mice, while no difference in tumor growth was detected compared with WT mice (11). Another study has shown that tumor growth in pericyte-deficient $Pdgfb^{ret/ret}$ mice may be increased or unchanged, depending on the specific tumor type (41). Enhanced tumor growth in $Pdgfb^{ret/ret}$ mice was connected to an accumulation of immunosuppressive myeloid-derived suppressor cells in the tumor tissue, caused by hypoxia-induced upregulation of IL6 (42).

Spontaneous metastasis was enhanced in RT2 and HCmel12 mice with PDGFB-deficient platelets, measured as nodules/tissue section, and we found an elevated level of CTCs in pl-PDGFB–KO RT2 mice. However, when tumor cells were injected directly in the circulation, no difference in experimental lung metastasis was found between WT and pl-PDGFB–KO mice. These data indicate that the increase in metastasis in pl-PDGFB–KO mice is because of increased intravasation of tumor cells. This finding could potentially be explained by a disrupted endothelial barrier in pericyte-deficient tumor vasculature in pl-PDGFB–KO mice, facilitating tumor cell passage. Pericyte-deficient vessels can also create a hypoxic microenvironment (42), which can drive EMT and invasive behavior of malignant cells (32, 33). A role for pericytes in limiting metastases in RT2 mice was previously reported by Xian and colleagues (43), showing that RT2 mice on the pericyte-deficient $Pdgfb^{ret/ret}$ background display enhanced metastasis and leaky vasculature. In two studies using pericyte ablation, it was shown that pericytes can limit hypoxia-induced EMT and metastasis (44, 45). In human colorectal carcinoma, increased metastatic events were found to correlate to low degree of pericyte coverage in the primary tumor (46). We could indeed detect elevated expression of hypoxia-inducible targets such as HIF1α, BNIP3, and CA9 in tumor tissue from pl-PDGFB–KO mice compared with WT, as well as a more mesenchymal tumor phenotype, based on the expression levels of E-cadherin, ZO-1, and vimentin. These changes in the primary tumor likely explains the enhanced intravasation of tumor cells in pl-PDGFB–KO mice.

Collectively, our data suggest that specific platelet granule proteins like PDGF help to preserve vascular integrity in tumors, and most likely during wound healing, thus limiting metastasis. This is in contrast to the well-described overall prometastatic properties of platelets (47).

The *Pf4-Cre* mice contain an extra copy of the *Cxcl3, Cxcl5, Cxcl7*, and *Cxcl15* genes (23). To rule out that increased expression of these chemokines plays a role in the effects reported in this study, we have analyzed the expression in tumor tissue from $Pf4\text{-}Cre^+$ and $Pf4\text{-}Cre^-$ RT2 mice. We could not detect any difference in expression levels of *Cxcl3, Cxcl5, Cxcl7*, and *Cxcl15* between the two genotypes (Supplementary Fig. S8A–S8D).

The receptor for PDGFB on pericytes, PDGFRβ, has an additional ligand in the PDGF family of growth factors, namely PDGFD (48, 49). Similar to PDGFB, PDGFD is expressed by the endothelium (50, 51). In contrast to PDGFB, total knockout of PDGFD generates viable and fertile offspring, but with a mild vascular phenotype, including disorganized $NG2^+$ pericytes in cardiac vessels (51). When crossed to the RT2 model, tumor growth was inhibited both in $Pdgfd^{+/-}$ and $Pdgfd^{-/-}$ mice, a finding that was attributed to lack of stimulation of a small subpopulation of PDGFRβ-positive tumor cells (52). Pericyte recruitment was, however, not impaired in RT2 tumors in PDGFD-deficient mice, which indicates a specific role of PDGFB in this context. It was speculated that the lack of a retention motif in PDGFD could enable this growth factor to travel further from the vasculature and therefore target other cell types (52). Whether PDGFD is present in platelets remains to be demonstrated, but on the basis of the above data, it is unlikely that PDGFD could compensate for the lack of PDGFB in pericyte recruitment.

Complete knockout of PDGFB in mice is embryonically lethal due to microvascular bleedings caused by lack of pericytes and vascular smooth muscle cells (6, 28). Conditional knockout of PDGFB under the control of the Tie 1 promotor generates viable and fertile offspring with a varying degree of pericyte coverage in the vasculature (8, 9). Tie 1 is expressed in endothelial cells, but its expression has also been reported in hematopoietic cells (53–55). If, or to what degree, PDGFB expression in megakaryocytes and platelets is affected in Tie 1–directed conditional knockout of PDGFB is currently unknown.

Despite the large collection of growth factors and other types of molecules stored in platelet granules, their individual roles in physiologic or pathologic situations are largely unexplored. One exception is TGFβ that was conditionally knocked out from platelets using the PF4 promoter (35). A study by Labelle and colleagues demonstrated that platelet-derived TGFβ plays a crucial role in promoting EMT and metastasis in cancer. It has been assumed that PDGFB secreted by activated platelets upon injury contributes to wound healing and tissue regeneration, but this remains to be demonstrated.

PDGFB secreted from activated platelets likely adds to the deposits of this growth factor in the ECM surrounding the vasculature and, thus, contributes to the vascular PDGFB gradient, required for proper recruitment of pericytes. This finding represents a novel mechanism describing how activated platelets can help to preserve the endothelial barrier in actively remodeling vasculature.

Disclosure of Potential Conflicts of Interest

C. Betsholtz reports grants from Swedish Cancer Foundation, Swedish Science Council, and Knut and Alice Wallenberg Foundation during the conduct of the study. A.-K. Olsson reports grants from The Swedish Cancer Society, The Swedish Research Council, and Ruth and Nils-Erik Stenbäck Foundation during the conduct of the study. No potential conflicts of interest were disclosed by the other authors.

Authors' Contributions

Y. Zhang: Conceptualization, formal analysis, supervision, investigation, visualization, methodology, writing-original draft, writing-review and editing. **J. Cedervall:** Conceptualization, formal analysis, supervision, investigation, visualization, writing-original draft, writing-review and editing. **A. Hamidi:** Formal analysis, investigation, visualization, writing-original draft. **M. Herre:** Formal analysis, investigation, visualization, writing-original draft. **K. Viitaniemi:** Formal analysis, investigation, visualization. **G. D'Amico:** Formal analysis, supervision, investigation, visualization. **Z. Miao:** Formal analysis, investigation. **R. Valsala Madhavan Unnithan:** Formal analysis, investigation. **A. Vaccaro:** Formal analysis, investigation. **L. van Hooren:** Formal analysis, investigation. **M. Georganaki:** Formal analysis, investigation. **Å. Thulin:** Formal analysis, investigation. **Q. Qiao:** Formal analysis, investigation. **J. Andrae:** Supervision, writing-review and editing. **A. Siegbahn:** Resources. **C.-H. Heldin:** Resources. **K. Alitalo:** Resources, supervision, methodology. **C. Betsholtz:** Supervision, methodology, writing-review and editing. **A. Dimberg:** Resources, supervision, writing-review and editing. **A.-K. Olsson:** Conceptualization, resources, formal analysis, supervision, funding acquisition, investigation, visualization, methodology, writing-original draft, project administration, writing-review and editing.

Acknowledgments

The *in situ* PLA experiments were performed at the PLA Proteomics facility, which is supported by Swedish Science for Life Laboratory. This work was supported by grants from The Swedish Cancer Society (CAN 2017/522), The Swedish Research Council (2016-03036), and Ruth and Nils-Erik Stenbäck Foundation (all to A.-K. Olsson).

The costs of publication of this article were defrayed in part by the payment of page charges. This article must therefore be hereby marked *advertisement* in accordance with 18 U.S.C. Section 1734 solely to indicate this fact.

Received November 8, 2019; revised April 24, 2020; accepted June 17, 2020; published first June 25, 2020.

References

1. Yuan SY, Rigor RR. Regulation of endothelial barrier function. San Rafael, CA: Morgan & Claypool Life Sciences; 2010.
2. Bergers G, Song S. The role of pericytes in blood-vessel formation and maintenance. Neuro Oncol 2005;7:452–64.
3. Gaengel K, Genove G, Armulik A, Betsholtz C. Endothelial-mural cell signaling in vascular development and angiogenesis. Arterioscler Thromb Vasc Biol 2009; 29:630–8.
4. Armulik A, Genove G, Betsholtz C. Pericytes: developmental, physiological, and pathological perspectives, problems, and promises. Dev Cell 2011;21: 193–215.
5. Soriano P. Abnormal kidney development and hematological disorders in PDGF beta-receptor mutant mice. Genes Dev 1994;8:1888–96.
6. Lindahl P, Johansson BR, Leveen P, Betsholtz C. Pericyte loss and microaneurysm formation in PDGF-B-deficient mice. Science 1997;277:242–5.
7. Hellstrom M, Kalen M, Lindahl P, Abramsson A, Betsholtz C. Role of PDGF-B and PDGFR-beta in recruitment of vascular smooth muscle cells and pericytes during embryonic blood vessel formation in the mouse. Development 1999;126: 3047–55.
8. Enge M, Bjarnegard M, Gerhardt H, Gustafsson E, Kalen M, Asker N, et al. Endothelium-specific platelet-derived growth factor-B ablation mimics diabetic retinopathy. EMBO J 2002;21:4307–16.
9. Bjarnegard M, Enge M, Norlin J, Gustafsdottir S, Fredriksson S, Abramsson A, et al. Endothelium-specific ablation of PDGFB leads to pericyte loss and glomerular, cardiac and placental abnormalities. Development 2004;131: 1847–57.
10. Lindblom P, Gerhardt H, Liebner S, Abramsson A, Enge M, Hellstrom M, et al. Endothelial PDGF-B retention is required for proper investment of pericytes in the microvessel wall. Genes Dev 2003;17:1835–40.
11. Abramsson A, Lindblom P, Betsholtz C. Endothelial and nonendothelial sources of PDGF-B regulate pericyte recruitment and influence vascular pattern formation in tumors. J Clin Invest 2003;112:1142–51.
12. Nystrom HC, Lindblom P, Wickman A, Andersson I, Norlin J, Faldt J, et al. Platelet-derived growth factor B retention is essential for development of normal structure and function of conduit vessels and capillaries. Cardiovasc Res 2006;71: 557–65.
13. Morikawa S, Baluk P, Kaidoh T, Haskell A, Jain RK, McDonald DM. Abnormalities in pericytes on blood vessels and endothelial sprouts in tumors. Am J Pathol 2002;160:985–1000.
14. Baluk P, Hashizume H, McDonald DM. Cellular abnormalities of blood vessels as targets in cancer. Curr Opin Genet Dev 2005;15:102–11.
15. Falcon BL, Hashizume H, Koumoutsakos P, Chou J, Bready JV, Coxon A, et al. Contrasting actions of selective inhibitors of angiopoietin-1 and angiopoietin-2 on the normalization of tumor blood vessels. Am J Pathol 2009;175:2159–70.
16. Cedervall J, Zhang Y, Ringvall M, Thulin A, Moustakas A, Jahnen-Dechent W, et al. HRG regulates tumor progression, epithelial to mesenchymal transition and metastasis via platelet-induced signaling in the pre-tumorigenic microenvironment. Angiogenesis 2013;16:889–902.
17. Ho-Tin-Noe B, Goerge T, Wagner DD. Platelets: guardians of tumor vasculature. Cancer Res 2009;69:5623–6.
18. Ho-Tin-Noe B, Goerge T, Cifuni SM, Duerschmied D, Wagner DD. Platelet granule secretion continuously prevents intratumor hemorrhage. Cancer Res 2008;68:6851–8.
19. Kisucka J, Butterfield CE, Duda DG, Eichenberger SC, Saffaripour S, Ware J, et al. Platelets and platelet adhesion support angiogenesis while preventing excessive hemorrhage. Proc Natl Acad Sci U S A 2006;103:855–60.

20. Versteeg HH. Tissue factor: old and new links with cancer biology. Semin Thromb Hemost 2015;41:747–55.
21. Lip GY, Chin BS, Blann AD. Cancer and the prothrombotic state. Lancet Oncol 2002;3:27–34.
22. Workman P, Balmain A, Hickman JA, McNally NJ, Rohas AM, Mitchison NA, et al. UKCCCR guidelines for the welfare of animals in experimental neoplasia. Lab Anim 1988;22:195–201.
23. Tiedt R, Schomber T, Hao-Shen H, Skoda RC. Pf4-Cre transgenic mice allow the generation of lineage-restricted gene knockouts for studying megakaryocyte and platelet function *in vivo*. Blood 2007;109:1503–6.
24. Ringvall M, Thulin A, Zhang L, Cedervall J, Tsuchida-Straeten N, Jahnen-Dechent W, et al. Enhanced platelet activation mediates the accelerated angiogenic switch in mice lacking histidine-rich glycoprotein. PLoS One 2011;6:e14526.
25. van Kuppeveld FJ, Johansson KE, Galama JM, Kissing J, Bolske G, van der Logt JT, et al. Detection of mycoplasma contamination in cell cultures by a mycoplasma group-specific PCR. Appl Environ Microbiol 1994;60:149–52.
26. Bald T, Quast T, Landsberg J, Rogava M, Glodde N, Lopez-Ramos D, et al. Ultraviolet-radiation-induced inflammation promotes angiotropism and metastasis in melanoma. Nature 2014;507:109–13.
27. Soderberg O, Gullberg M, Jarvius M, Ridderstrale K, Leuchowius KJ, Jarvius J, et al. Direct observation of individual endogenous protein complexes *in situ* by proximity ligation. Nat Methods 2006;3:995–1000.
28. Leveen P, Pekny M, Gebre-Medhin S, Swolin B, Larsson E, Betsholtz C. Mice deficient for PDGF B show renal, cardiovascular, and hematological abnormalities. Genes Dev 1994;8:1875–87.
29. Bergers G, Javaherian K, Lo KM, Folkman J, Hanahan D. Effects of angiogenesis inhibitors on multistage carcinogenesis in mice. Science 1999;284:808–12.
30. Folkman J, Watson K, Ingber D, Hanahan D. Induction of angiogenesis during the transition from hyperplasia to neoplasia. Nature 1989;339:58–61.
31. Inoue M, Hager JH, Ferrara N, Gerber HP, Hanahan D. VEGF-A has a critical, nonredundant role in angiogenic switching and pancreatic beta cell carcinogenesis. Cancer Cell 2002;1:193–202.
32. Ebos JM, Lee CR, Cruz-Munoz W, Bjarnason GA, Christensen JG, Kerbel RS. Accelerated metastasis after short-term treatment with a potent inhibitor of tumor angiogenesis. Cancer Cell 2009;15:232–9.
33. Paez-Ribes M, Allen E, Hudock J, Takeda T, Okuyama H, Vinals F, et al. Antiangiogenic therapy elicits malignant progression of tumors to increased local invasion and distant metastasis. Cancer Cell 2009;15:220–31.
34. Mellor HR, Harris AL. The role of the hypoxia-inducible BH3-only proteins BNIP3 and BNIP3L in cancer. Cancer Metastasis Rev 2007;26:553–66.
35. Labelle M, Begum S, Hynes RO. Direct signaling between platelets and cancer cells induces an epithelial-mesenchymal-like transition and promotes metastasis. Cancer Cell 2011;20:576–90.
36. Heldin CH, Westermark B, Wasteson A. Platelet-derived growth factor: purification and partial characterization. Proc Natl Acad Sci U S A 1979;76:3722–6.
37. Kaminski WE, Lindahl P, Lin NL, Broudy VC, Crosby JR, Hellstrom M, et al. Basis of hematopoietic defects in platelet-derived growth factor (PDGF)-B and PDGF beta-receptor null mice. Blood 2001;97:1990–8.
38. Verheul HM, Hoekman K, Luykx-de Bakker S, Eekman CA, Folman CC, Broxterman HJ, et al. Platelet: transporter of vascular endothelial growth factor. Clin Cancer Res 1997;3:2187–90.
39. Blakytny R, Ludlow A, Martin GE, Ireland G, Lund LR, Ferguson MW, et al. Latent TGF-beta1 activation by platelets. J Cell Physiol 2004;199:67–76.
40. Dvorak HF. Tumors: wounds that do not heal. Similarities between tumor stroma generation and wound healing. N Engl J Med 1986;315:1650–9.
41. Nisancioglu MH, Betsholtz C, Genove G. The absence of pericytes does not increase the sensitivity of tumor vasculature to vascular endothelial growth factor-A blockade. Cancer Res 2010;70:5109–15.
42. Hong J, Tobin NP, Rundqvist H, Li T, Lavergne M, Garcia-Ibanez Y, et al. Role of tumor pericytes in the recruitment of myeloid-derived suppressor cells. J Natl Cancer Inst 2015;107:djv209.
43. Xian X, Hakansson J, Stahlberg A, Lindblom P, Betsholtz C, Gerhardt H, et al. Pericytes limit tumor cell metastasis. J Clin Invest 2006;116:642–51.
44. Cooke VG, LeBleu VS, Keskin D, Khan Z, O'Connell JT, Teng Y, et al. Pericyte depletion results in hypoxia-associated epithelial-to-mesenchymal transition and metastasis mediated by met signaling pathway. Cancer Cell 2012;21:66–81.
45. Keskin D, Kim J, Cooke VG, Wu CC, Sugimoto H, Gu C, et al. Targeting vascular pericytes in hypoxic tumors increases lung metastasis via angiopoietin-2. Cell Rep 2015;10:1066–81.
46. Yonenaga Y, Mori A, Onodera H, Yasuda S, Oe H, Fujimoto A, et al. Absence of smooth muscle actin-positive pericyte coverage of tumor vessels correlates with hematogenous metastasis and prognosis of colorectal cancer patients. Oncology 2005;69:159–66.
47. Felding-Habermann B, Habermann R, Saldivar E, Ruggeri ZM. Role of beta3 integrins in melanoma cell adhesion to activated platelets under flow. J Biol Chem 1996;271:5892–900.
48. Bergsten E, Uutela M, Li X, Pietras K, Ostman A, Heldin CH, et al. PDGF-D is a specific, protease-activated ligand for the PDGF beta-receptor. Nat Cell Biol 2001;3:512–6.
49. LaRochelle WJ, Jeffers M, McDonald WF, Chillakuru RA, Giese NA, Lokker NA, et al. PDGF-D, a new protease-activated growth factor. Nat Cell Biol 2001;3:517–21.
50. Bergers G, Song S, Meyer-Morse N, Bergsland E, Hanahan D. Benefits of targeting both pericytes and endothelial cells in the tumor vasculature with kinase inhibitors. J Clin Invest 2003;111:1287–95.
51. Gladh H, Folestad EB, Muhl L, Ehnman M, Tannenberg P, Lawrence AL, et al. Mice lacking platelet-derived growth factor d display a mild vascular phenotype. PLoS One 2016;11:e0152276.
52. Cortez E, Gladh H, Braun S, Bocci M, Cordero E, Bjorkstrom NK, et al. Functional malignant cell heterogeneity in pancreatic neuroendocrine tumors revealed by targeting of PDGF-DD. Proc Natl Acad Sci U S A 2016;113:E864–73.
53. Rodewald HR, Sato TN. Tie1, a receptor tyrosine kinase essential for vascular endothelial cell integrity, is not critical for the development of hematopoietic cells. Oncogene 1996;12:397–404.
54. Tsiamis AC, Hayes P, Box H, Goodall AH, Bell PR, Brindle NP. Characterization and regulation of the receptor tyrosine kinase Tie-1 in platelets. J Vasc Res 2000;37:437–42.
55. Gustafsson E, Brakebusch C, Hietanen K, Fassler R. Tie-1-directed expression of Cre recombinase in endothelial cells of embryoid bodies and transgenic mice. J Cell Sci 2001;114:671–6.